**Advances in
Radio Science**

Leaky wave antenna with amplitude controlled beam steering based on composite right/left-handed transmission lines

M. A. Eberspächer and T. F. Eibert

Lehrstuhl für Hochfrequenztechnik, Technische Universität München, Germany

Abstract. An antenna comprising two different composite right/left-handed transmission line structures is proposed which enables easy beam steering at an operation frequency of 10 GHz. The composite right/left-handed transmission lines are based on planar, periodically arranged via free unit cells, implemented in microstrip technology. Both transmission lines exhibit the infinite wavelength phenomenon which occurs at 9.72 GHz and 9.89 GHz, respectively. Thus, operating the different leaky wave structures at 10 GHz, radiation with azimuth angles of $\pm 8°$ and $\pm 17°$ can be achieved depending on the selected input port. In order to obtain a tunable main beam direction, the radiation patterns of both structures are superimposed by feeding them simultaneously. The influence of each guiding structure, and hence the direction of the main beam, can be controlled via the feeding amplitude. As a result of this, the beam can be steered between $\pm 17°$ with a gain of up to 10 dBi. The guiding structures are arranged in parallel with a clearance of $a = 12.2$ mm which is less than half of the wavelength in free space. This allows in a further step the attachment of additional guiding structures in order to increase the tunable angle range or creating an antenna array with a small beamwidth in the elevation plane without the occurrence of grating lobes. An antenna prototype was fabricated and validated by measurements.

1 Introduction

Since the advent of automotive radar systems, highly directive antennas supporting easy beam steering have received considerable attention. As shown in Balanis (2005), the beamwidth of an antenna becomes smaller when its aperture is increased. Thus, realising a small beamwidth requires a

sufficiently large aperture. Travelling wave antennas are attractive candidates for this type of application due to the fact, that their aperture sizes do not adhere with the operation frequency, and hence the aperture can be chosen almost arbitrarily. The mapping between frequency and radiation direction of the antenna can be controlled during the design process by dispersion engineering (Walter, 1965). However, the main beam direction of a leaky wave antenna is tightly coupled to the operation frequency and cannot be changed dynamically. Thus, many research efforts have been done and versatile concepts have been presented to allow beam steering at a constant frequency, for example with a rotating dielectric grating structure as in Schneider and Wenger (2003), with a movable dielectric slab as in Matsuzawa et al. (2006), or by using lens antennas as in Binzer et al. (2007). All these presented structures are proven to work well, however, their realisation and production is very costly.

2 Theory

2.1 Principle of leakage radiation

A leaky wave is a travelling wave which progressively leaks out power as it propagates along a waveguiding structure (Caloz and Itoh, 2006). Consequently, a structure supporting one or more leaky waves is referred to as leaky wave structure. In the following, a planar waveguide located in the xy-pane is considered. The waveguide supports an electromagnetic wave travelling along the structure in the x-direction. By suppressing the time dependency, this wave can be described as $\psi(x) = \psi_0 e^{-\gamma x}$, where $\gamma = \alpha + \mathrm{j}\beta$ represents its complex propagation constant. The field above the guiding structure which is excited by the travelling wave can be written as

$$\psi(x,z) = \psi_0 e^{-\gamma x} e^{-\mathrm{j}k_z z}. \tag{1}$$
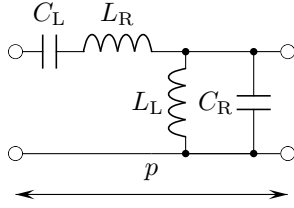
Fig. 1. Equivalent circuit of a CRLH TL unit cell with series impedance $Z = j\omega L_R + \frac{1}{j\omega C_L}$ and the parallel admittance $Y = j\omega C_R + \frac{1}{j\omega L_L}$.

In order to fulfill Maxwell's equations, the wavenumber in z-direction is given as

$$k_z = \sqrt{k_0^2 - (\beta - j\alpha)^2}, \quad (2)$$

where $k_0 = \omega/c$ is the free space wavenumber. If we consider a lossless antenna with relatively small leakage, α can be neglected and the wavenumber simplifies to $k_z = \sqrt{k_0^2 - \beta^2}$. Depending on β, this leads either to a purely imaginary k_z or a purely real k_z. Accordingly, the first case represents an evanescent wave exponentially decaying whereas the latter stands for leakage radiation.

The main beam direction of this leakage radiation can be calculated as shown in Walter (1965) according to

$$\Theta_{MB} = \arcsin \frac{\beta(\omega)}{k_0}. \quad (3)$$

Analysing the argument of the angular function yields that a real angle can only be found for $|\beta(\omega)| \le k_0$. This accords exactly to the prerequisites in Eq. (2) for a purely real propagation constant k_z.

The relationship between the beamwidth Θ_{BW} and the aperture length L of the leaky wave antenna is given in Johnson (1993) by

$$\Theta_{BW} \approx \frac{1}{(L/\lambda_0)\cos\Theta_{MB}}. \quad (4)$$

For a given value of α, the antenna length L is usually chosen so that approximately 90% of the power is radiated. As expected, the beamwidth becomes smaller for a longer aperture.

2.2 Artificial transmission line theory

In order to design leaky wave antennas with predefined behaviour, guiding structures with certain dispersion characteristics are required. A very powerful approach to accomplish this are periodic structures. This type of structures are composed of periodically arranged small sections, which can be considered as unit cells. It is shown that the analysis of the whole structure can be restricted to the analysis of one unit cell (Pozar, 2005). Hence, in the ideal case also the design

process of a guiding structure is reduced to the design effort of a single cell. The dispersion behaviour of such a guiding structure is given by

$$(\alpha + j\beta)p = \operatorname{arccosh} \frac{A+D}{2}, \quad (5)$$

where p stands for the physical length of the unit cell and the parameters A and D are its elements of the ABCD-Matrix representation. Since the result of the arccosh-function is ambiguous, the phase constant has multiple solutions $\beta_n p = \beta_0 p + \frac{2\pi n}{p}$ with $n = 0, \pm 1, \pm 2, \pm 3, \dots$. Besides the fundamental mode β_0, an infinite number of so-called space harmonics are obtained. In general, a structure can be designed in such a way that either radiation occurs at the fundamental mode or at any arbitrarily chosen space harmonic as long as Eq. (3) leads to a real angle Θ_{MB}. However, as it is mentioned in Paulotto et al. (2008) radiation at broadside using space harmonics can be disturbed due to coupling effects of a pair of these harmonics resulting in an open stop band. This problem can be overcome by radiating only with the fundamental mode. Consequently, β_0 is forced to be zero to achieve broadside radiation at a certain frequency $\omega \ne 0$, which can be realised by using composite right/left-handed (CRLH) transmission lines.

As shown in Fig. 1, the CRLH-unit cell is composed of a series and a parallel resonant circuit with the resonant frequencies ω_s and ω_p, respectively. In both resonant circuits the elements denoted with index L are accountable for the left-handed behaviour of the arrangement. On the other hand, components with index R make the unit cell to behave as right-handed. According to the equivalent circuit of a conventional transmission line, the right-handed contributions can be implemented either as lumped elements or as sections of transmission lines. Additionally, the occurring parasitics can be included in these elements.

Calculating the corresponding ABCD-Matrix elements of the circuit in Fig. 1, inserting them in Eq. (5), and performing a taylor series expansion yields $j\beta = \frac{\sqrt{YZ}}{p}$. It is shown in Caloz and Itoh (2006), that $\beta = \Re\{\beta\}$, if $\omega_s = \omega_p$, and hence no stop band occurs. This case is referred to as the balanced case in which the phase constant is written as $j\beta = \frac{j}{p} \left(\omega\sqrt{L_R C_R} - \frac{1}{\omega\sqrt{C_L L_L}} \right)$. Obviously, a given value of the phase constant at a certain frequency can be realised by choosing the appropriate network elements L_R, C_R, L_L and L_L. Thus, it is possible to create a leaky wave structure possessing a certain main beam direction at a given frequency.

The counterpart of the characteristic impedance of a homogeneous transmission line is the Bloch impedance of a periodic artificial structure. In contrast to the characteristic impedance, the latter is usually given at the terminals of the unit cell only. According to Pozar (2005), the Bloch impedance can be determined based on the ABCD-Matrix elements as
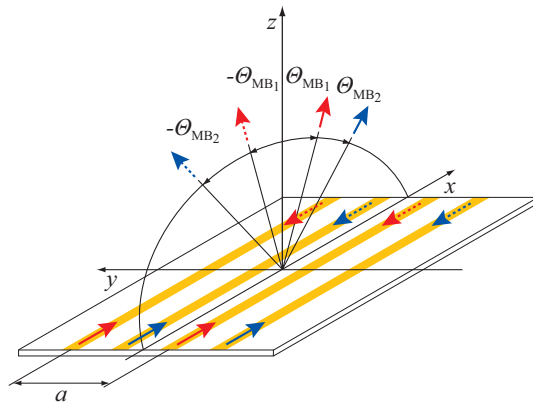
$$Z_L = \sqrt{\frac{Z}{Y}}. \quad (6)$$

Fig. 2. Arrangement of two times two identical leaky wave structures. Excitation according to the red solid and dashed arrow leads to main beam direction Θ_{MB1} and $-\Theta_{MB1}$, respectively. Excitation according to the blue solid and dashed arrow leads to main beam direction Θ_{MB2} and $-\Theta_{MB2}$, respectively.

Applying Eq. (6) to the circuit in Fig. 1 results in the frequency independent Bloch impedance $Z_L = \sqrt{\frac{L_L}{C_L}} = \sqrt{\frac{L_R}{C_R}}$.

2.3 Concept of beam steering

Naturally, the main beam direction of a leaky wave antenna can be steered by changing its operation frequency. However, a concept allowing different main beam directions at a constant frequency is investigated in this work.

To clarify the basic idea, let us consider a leaky wave structure with two ports located at their opposite ends. The ports are referred to as port 1 and port 2, respectively. Operating the structure at the frequency $f_0 = \omega_0/2\pi \neq 0$ at port 1, a leakage mode is excited which propagates along the structure to port 2 at which it is supposed to be absorbed. Thus, radiation occurs with an azimuth main beam Θ_{MB1} according to Eq. (3) and the propagation constant of the excited mode. The structure can be designed in such a way that this angle $\Theta_{MB1} \neq 0$ at the frequency f_0.

If the driven port and the terminated port are interchanged, the phase constant will be negative with respect to port 1 and hence, radiation with the main beam direction $-\Theta_{MB1}$ will occur. As it is seen in Eq. (4), the beamwidth Θ_{BW1} of the antenna in the azimuth plane is determined by the aperture length L. Thus, the beamwidth can be manipulated by the amount of cascaded unit cells along the x-axis.

Further main beam angles are achievable by adding other leaky wave structures in parallel which possess the angles $\pm\Theta_{MBn}$. This can be done any number of times if the beamwidth in the elevation (yz-) plane can be broad. However, the requirement of a small beamwidth in this plane limits this approach, since leaky wave structures exhibiting the same azimuth angle must be repeated periodically. Figure 2 shows such an arrangement of two times two leaky wave
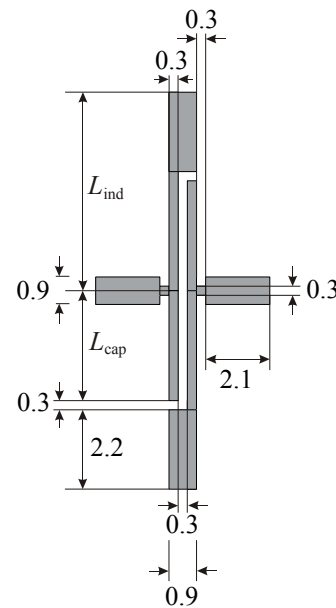
Structure 1:
$f = 9.72$ GHz
$L_{ind} = 6.45$
$L_{cap} = 3.95$

Structure 2:
$f = 9.89$ GHz
$L_{ind} = 6.35$
$L_{cap} = 3.85$

Substrate :
Taconic TLY-5
thickness = 0.78
DK = 2.2
DF = 0.0009

Dimensions:
mm

Fig. 3. Layout of the two realised unit cells.

structures. Structures possessing the same main beam direction are marked with arrows of the same colour. The distance between identical antennas is a. In order to avoid grating lobes in the yz-plane, a has to be smaller than λ_0 for radiation in the upper hemisphere only. This limitation makes the design process troublesome, since reducing the clearance leads to increased mutual coupling. The increase of the coupling effects can grow up to such an extent that the structure becomes inoperative.

According to the antenna depicted in Fig. 2, there are four different main beam directions possible, which can be chosen via the corresponding feeding. An excitation of the antenna according to the red solid and dashed arrows leads to radiation into the direction of Θ_{MB1} and $-\Theta_{MB1}$, respectively. The angles Θ_{MB2} and $-\Theta_{MB2}$ can be adjusted by feeding according to the blue solid and dashed arrows, respectively.

Furthermore, the radiation patterns of two structures can be superimposed by feeding them simultaneously in order to gain additional main beam directions. The influence of each guiding structure, and hence the direction of the main beam, can be controlled via the feeding amplitude. To ensure that each combination leads to only one main beam, the particular patterns have to fulfill

$$\Theta_{MB1} + \Theta_{BW1}/2 \geq \Theta_{MB2} - \Theta_{BW2} \qquad (7)$$

with $\Theta_{MB1} \leq \Theta_{MB2}$.

3 Realisation

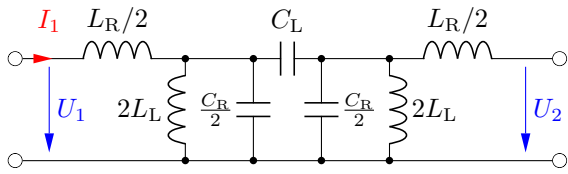The aim is to create an antenna comprising two different leaky wave structures, which possess at the operation

Fig. 4. Simplified equivalent circuit model of the realised unit cell with neglected losses.

Fig. 6. Fabricated leaky wave structures. The numbers are indicating the ports.
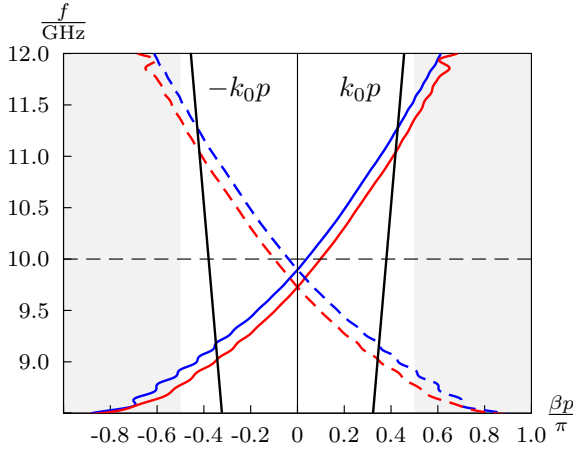

Fig. 5. Dispersion diagram of the unit cells with the transition frequencies $f_1 = 9.72$ GHz (red line) and $f_2 = 9.89$ GHz (blue line). At 10 GHz the unit cells exhibit a phase constant of $\beta_1 = 0.098\frac{\pi}{p}$ and $\beta_2 = 0.038\frac{\pi}{p}$, respectively.

Fig. 7. Measured S-parameters of the leaky wave structures: S_{11} blue line, S_{21} black line, S_{33} red dashed line and S_{43} orange dashed line.

frequency of 10 GHz the main beam directions Θ_{MB1} and Θ_{MB2}, respectively. In order to allow the extension of the aperture in y-direction subsequently, the distance between adjacent structures should be less than $\lambda_0/2$. Furthermore, an easy to fabricate design is wanted which can be produced using a standard photolithography process.

The unit cell presented in Eberspächer et al. (2009) is easily realisable and needs neither an interlayer connection nor a multilayer fabrication process. Hence, it can be produced in an entirely printed circuit technology. Consequently, the concept of this unit cell is taken as a basis for this antenna design. However, it cannot be implemented directly, since strong mutual coupling between adjacent leaky wave structures occurs. Therefore, the unit cell must be narrowed in y-direction without changing the electromagnetic behaviour. This means that the open ended inductive stubs must be shortened while the electrical length must be unchanged. This can be achieved by introducing impedance steps along the stub. Beginning at the open end, a stepwise change of the characteristic impedance from a low to a high level is required. In microstrip technology, this is easily achieved by a step in the width of the line. The resulting design is shown in Fig. 3.

In the next step, the unit cells were balanced upon the transition frequencies 9.72 GHz and 9.89 GHz. According to
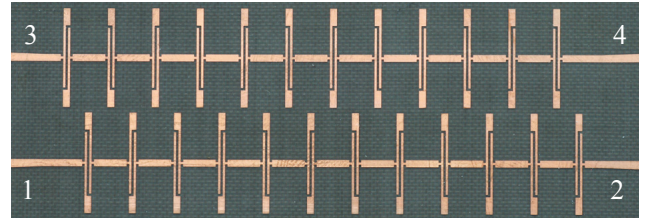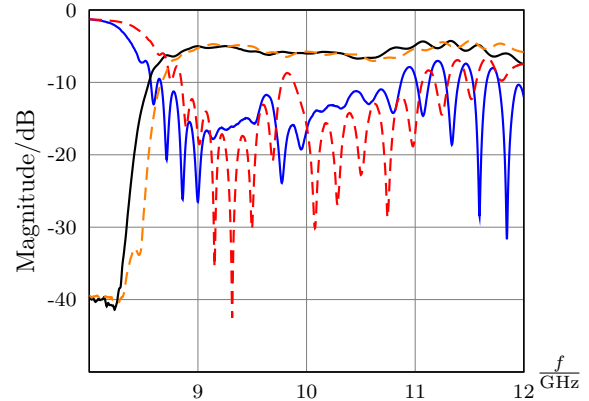
the dispersion diagram seen in Fig. 5, one obtains the phase constants of $\beta_1(2\pi\, 10\,\text{GHz}) = 0.098\frac{\pi}{p}$ and $\beta_2(2\pi\, 10\,\text{GHz}) = 0.038\frac{\pi}{p}$, respectively. Employing Eq. (3), this leads theoretically to the main beam directions $\Theta_{MB1} = 15°$ and $\Theta_{MB2} = 5.8°$. Balancing a unit cell consisting of discrete elements can be done easily by choosing the appropriate values. However, the proposed cell requires a more sophisticated balancing procedure. Therefore, information are required which describe whether the unit cell is balanced or not. Furthermore, it is important to know, which resonant circuit should be tuned. These information are provided by the **Z** and **Y** matrix elements obtained by the numerical computation software CST Microwave Studio (CST).

During the balancing process of the structure losses are not considered. According to the resulting simplified equivalent circuit model, seen in Fig. 4, the element Z_{21} can be calculated analytically. Per definition $Z_{21} = \frac{U_2}{I_1}\big|_{I_2=0}$. From this follows that neither of the series inductances must be taken into account. Thus, this impedance reads

$$Z_{21} = \frac{j\omega^3 4L_L^2 C_L}{(1 - \omega^2 L_L C_R)(1 - \omega^2 L_L C_R - \omega^2 4 C_L L_L)}. \quad (8)$$

Searching for roots of the denominator gives
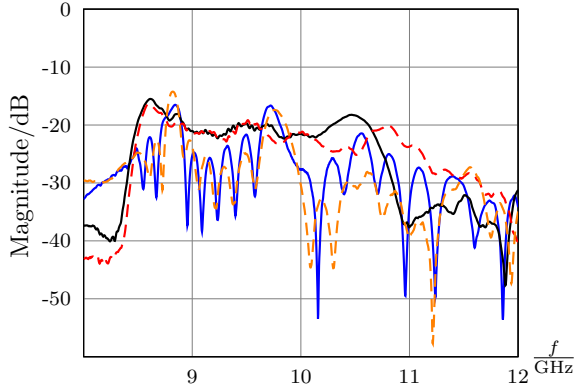
$$\omega_{fp} = \sqrt{\frac{1}{(C_R + 4C_L)L_L}}$$

Fig. 8. Measured S-parameters of the leaky wave structures: S_{31} blue line, S_{41} black line, S_{32} red dashed line and S_{42} orange dashed line.
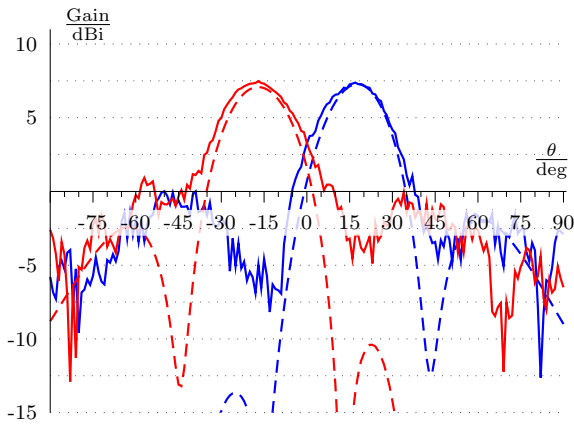

Fig. 9. Radiation pattern in the xz-plane (x-direction polarised). Measurement and simulation results are drawn in solid lines and dashed lines, respectively. Excitation at port 1 (blue line) and at port 2 (red line).

Fig. 10. Radiation pattern in the xz-plane (x-direction polarised). Measurement and simulation results are drawn in solid lines and dashed lines, respectively. Excitation at port 2 (blue line) and at port 4 (red line).
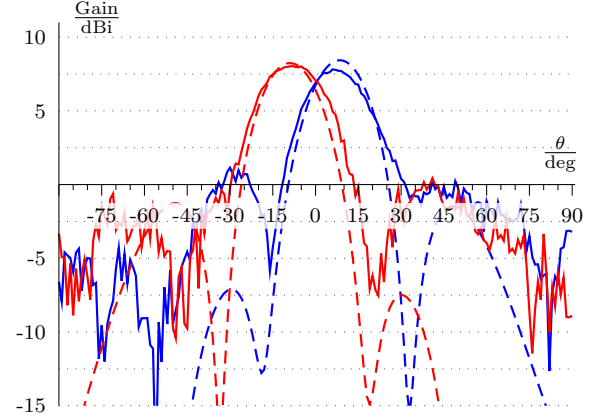

Fig. 11. Radiation pattern in the xz-plane (x-direction polarised). Measurement and simulation results are drawn in solid lines and dashed lines, respectively. Excitation at port 1+3 (blue line) and at port 2+4 (red line).
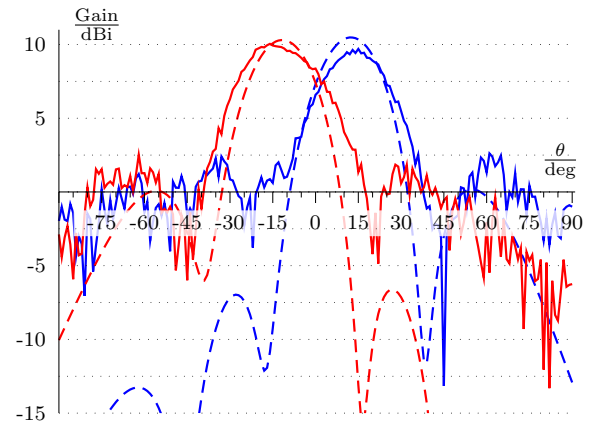
and

$$\omega_{f p_{res}} = \sqrt{\frac{1}{L_L C_R}}.$$

Since $C_L > 0$, it is found that $\omega_{fp} < \omega_{fp_{\mathrm{res}}}$. The numerator is unequal to zero at both frequencies which leads to two maxima of $|Z_{21}|$. The position of the peak occurring at the higher frequency identifies the parallel resonant frequency.

Determining the series resonant frequency can be done based on Y_{11}. With the prerequisites that the parallel resonant frequency is tuned correctly, its conductance is insignificant around this frequency. Thus, the admittance matrix element simplifies to

$$Y_{11} = \left. \frac{I_1}{U_1} \right|_{U_2=0} \approx \frac{j \omega L_R}{1 - \omega^2 L_R C_L}. \tag{9}$$

Only one maxima can be found for $|Y_{11}|$ which identifies exactly the series resonant frequency $\omega_{f s_{\mathrm{res}}} = \sqrt{\frac{1}{L_R C_L}}$. Follow-

ing these steps, both unit cells were balanced and tuned correctly to the desired frequencies. Their exact dimensions are shown in Fig. 3.

It should be mentioned, that due to mutual coupling the behaviour of a cascaded unit cell changes and detuning occurs. Thus, it is advisable to determine the elements Y_{11} and Z_{21} out of a cascaded arrangement by performing a deembedding process.

4   Results

The designed structure was fabricated, as seen in Fig. 6, and successfully tested. The measured reflection and transmission coefficients are shown in Fig. 7. Additional measurements were done determining the mutual coupling. As
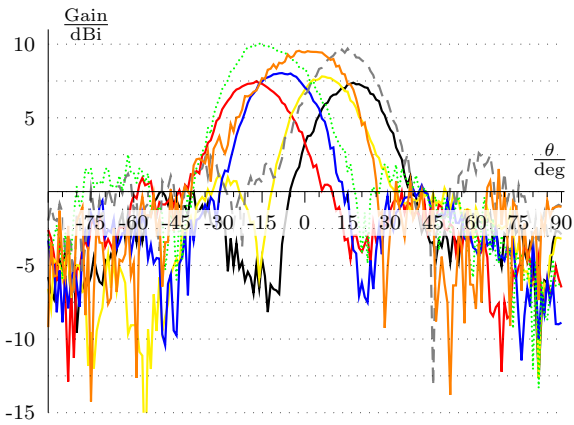
Fig. 12. Measured radiation pattern in the xz-plane (x-direction polarised). Excitation and colors are related as follows: Port 1 black, port 2 red, port 3 yellow, port 4 blue, port 1+3 gray dashed, port 2+4 green dotted, port 3+4 orange. Detailed pattern information are given in Table 1.

Table 1. Measured radiation pattern characteristics of the realised antenna.

Excitation	Gain	Θ_{MB}	Θ_{BW}
Port 1	7.4 dBi	17°	26°
Port 2	7.5 dBi	−17°	28°
Port 3	7.8 dBi	7°	25°
Port 4	8.0 dBi	−8°	27°
Port 1+3	9.7 dBi	14°	30°
Port 2+4	10.1 dBi	−15°	28°
Port 3+4	9.5 dBi	−1°	35°

shown in Fig. 8, this analysis yields an attenuation greater than 15 dB between neighbouring structures over a broad frequency range. The dispersion diagram obtained by simulation and the measured radiation patterns are depicted in Figs. 5, 9–12. Details of the achieved results are provided in Table 1. All parameters possess a good agreement with the analytical results from Eqs. (3) and (4). As expected, the gain increases when both structures are driven simultaneously, since the aperture in y-direction is enlarged. Consequently, the beamwidth in the yz-plane becomes smaller and gain enhancement takes place.

5 Conclusions

A beam steering concept was presented, which is based on two leaky wave structures with different main beam directions. The structures are realised as composite right/left-handed transmission lines with different transition frequencies. Thus, the main beam can be switched according to the chosen feeding port or steered by superimposing the different radiation patterns. The presented antenna possesses a scan angle range of $−17° ≤ 0 ≤ 17°$ with a gain of up to 10 dBi at the operation frequency of 10 GHz.

References

Balanis, C. A.: Antenna theory – analysis and design, John Wiley & Sons, 3rd edn., 2005.

Binzer, T., Klar, M., and Groß, V.: Development of 77 GHz Radar Lens Antennas for Automotive Applications Based on Given Requirements, 2nd International ITG Conference on Antennas, 2007.

Caloz, C. and Itoh, T.: Electromagnetic Metamaterials, John Wiley & Sons, 2006.

CST Computer Simulation Technology, http://www.cst.com/, access: 31 March 2010.

Eberspächer, M. A., Eccleston, K., and Eibert, T. F.: Realization of Via-free Microstrip Composite Right/Left-Handed Transmission Lines, Proceedings of the German Microwave Conference GeMiC 2009, 2009.

Johnson, R.: Antenna Engineering Handbook, chap. Leaky-Wave Antennas, McGraw Hill, 3rd edn., 1993.

Matsuzawa, S., Sato, K., Inoue, Y., and Nomura, T.: W-Band Steerable Composite Right/Left-Handed Leaky Wave Antenna for Automotive Applications, IEICE TRANSACTIONS on Electronics, 2006.

Paulotto, S., Baccarelli, P., Frezza, F., and Jackson, D. R.: Full-Wave Modal Dispersion Analysis and Broadside Optimization for a Class of Microstrip CRLH Leaky-Wave Antennas, IEEE Transaction on Microwave theory and techniques, 2008.

Pozar, D. M.: Microwave Engineering, John Wiley & Sons, 3rd edn., 2005.

Schneider, R. and Wenger, J.: High resolution radar for automobile applications, Adv. Radio Sci., 1, 105–111, 2003, http://www.adv-radio-sci.net/1/105/2003/.

Walter, C. H.: Traveling wave antennas, Dover, 1st edn., 1965.